

Article

Development of Small-Diameter Artificial Vascular Grafts Using Transgenic Silk Fibroin

Takashi Tanaka ^{1,*}, Sakiko Hara ¹, Hanan Hendawy ¹, Hussein M. El-Husseiny ^{1,2}, Ryo Tanaka ¹
and Tetsuo Asakura ³

¹ Department of Veterinary Science, Tokyo University of Agriculture and Technology, Tokyo 183-8509, Japan; sakiko.hara0515@gmail.com (S.H.); hanan_attia@vet.suez.edu.eg (H.H.); s195162s@st.go.tuat.ac.jp (H.M.E.-H.); ryo@vet.ne.jp (R.T.)

² Department of Surgery, Anesthesiology, and Radiology, Faculty of Veterinary Medicine, Benha University, Moshthor, Toukh 13736, Elqaliobiya, Egypt

³ Department of Biotechnology, Tokyo University of Agriculture and Technology, Tokyo 184-8588, Japan; asakura@cc.tuat.ac.jp

* Correspondence: bamse.rizea.vicky.polta@gmail.com; Tel.: +81-3-3935-3225

Abstract: Silk fibroin (SF) is a suitable material for vascular prostheses for small arteries. SF is useful not only as a base material for artificial vascular grafts but also as a coating material. This study prepared three types of transgenic SF (vascular endothelial growth factor (VEGF), Arg-Glu-Asp-Val (REDV), and Tyr-Ile-Gly-Ser-Arg (YIGSR)) incorporating expression factors that are thought to be effective for endothelialization as coating materials. We compared the contribution of these materials to early endothelialization in vivo when using them as a porous transgenic SF coating. A porous coating of transgenic SF containing VEGF, REDV, and YIGSR was applied to a silk small-diameter artificial vascular graft base with a diameter of 1.5 mm and a length of 3 cm. Two and four weeks after implantation of these artificial grafts into the abdominal aorta of rats, they were removed and evaluated by histologic examination. Transgenic SF coating incorporating VEGF and REDV demonstrated higher tissue infiltration and continuous endothelialization in the center of the graft compared to YIGSR at 4 weeks after implantation. VEGF and REDV are capable of endothelialization as early as 4 weeks after implantation, confirming the usefulness of transgenic SF when used as a porous coating.

Keywords: silk fibroin; small-diameter artificial vascular graft; vascular endothelial growth factor; REDV; YIGSR



Citation: Tanaka, T.; Hara, S.; Hendawy, H.; El-Husseiny, H.M.; Tanaka, R.; Asakura, T. Development of Small-Diameter Artificial Vascular Grafts Using Transgenic Silk Fibroin. *Prosthesis* **2023**, *5*, 763–773. <https://doi.org/10.3390/prosthesis5030054>

Academic Editors: Pablo Pennisi and Sandra Van Vlierberghe

Received: 12 July 2023

Revised: 10 August 2023

Accepted: 11 August 2023

Published: 12 August 2023



Copyright: © 2023 by the authors. Licensee MDPI, Basel, Switzerland. This article is an open access article distributed under the terms and conditions of the Creative Commons Attribution (CC BY) license (<https://creativecommons.org/licenses/by/4.0/>).

1. Introduction

Cardiovascular disease-related deaths occur in 17.3 million people globally each year, accounting for 30% of all deaths worldwide, with a predicted annual incidence of deaths to reach 23.3 million globally by 2030 [1]. Effective treatment for these diseases included replacement surgery using autologous blood vessels or artificial vascular grafts. Polyethylene terephthalate (PET) and expanded polytetrafluoroethylene (ePTFE) are widely applied clinically in large-diameter arteries (>10 mm), such as the thoracoabdominal aorta, and medium-diameter arteries (>6 mm), such as the neck and axillary regions. However, these materials obstruct due to intimal hyperplasia and thrombus when applied to small diameters (<6 mm) such as lower extremities and coronary arteries [2,3]. Replacement surgery using ePTFE has a low patency rate of 20% after 5 years [4]. Hence, autologous blood vessels can be used instead, but, at present, restrictions remain, such as the poor quality of the donor patient's blood vessels, the invasiveness of the resection surgery, and postoperative movement restrictions [5–7]. Therefore, the development of small-diameter artificial vascular grafts that do not occlude is desired.

Small-diameter artificial vascular grafts must meet various requirements to maintain long-term functionality. Thus, biocompatibility with surrounding tissues and adjacent autologous blood vessels should be obtained to not induce thrombosis, as well as appropriate mechanical strength and elasticity to withstand systolic blood pressure. We have been conducting studies for development toward clinical application because silk fibroin (SF) has the above properties and is considered a suitable material for small-diameter artificial vascular grafts. Previous studies revealed that artificial vascular grafts with silk fibroin as a base maintained patency in the abdominal aorta of rats for over one year after implantation and that the patency rate was higher than that of artificial vascular grafts using ePTFE. Additionally, graft remodeling due to biodegradation, which is one of the characteristics of SF, was confirmed [8]. The usefulness of SF in artificial vascular grafts is not limited to its use as a base. The small-diameter artificial vascular graft with SF coating applied to the SF base not only prevents blood leakage but also contributes to remodeling [9]. However, 15–30% of vessels after coronary artery bypass surgery are occluded in the first year after autologous vein implantation, and half of them are occluded in the first month [10]. Therefore, endothelialization at an early stage after implantation is desirable for practical use. This study aimed for early tissue infiltration and endothelialization by using genetically modified silk fibroin, in which a factor that promotes cell adhesion was introduced into the SF used for coating.

Vascular endothelial growth factor (VEGF) promotes vascular endothelial cell proliferation and induces angiogenesis [11]. In addition, platelet-derived growth factor (PDGF) inhibition suppressing excessive vascular smooth muscle cell proliferation, thereby suppressing intimal hyperplasia [12]. VEGF is used in medical materials such as stents and artificial vascular grafts because of these properties [13,14]. Fibronectin is a glycoprotein that forms the extracellular matrix, and Arg-Glu-Asp-Val (REDV), which is one of the active sites of cell adhesion, specifically recognizes integrin $\alpha 4\beta 1$ expressed in vascular endothelial cells and vascular endothelial progenitor cells [15]. Endothelialization was observed 1 week after implantation into pigs when the luminal surface of decellularized ostrich carotid arteries was modified with REDV, indicating that REDV is expected to induce early endothelialization of small-diameter artificial vascular grafts [16]. Laminin is one of the glycoproteins that constitute the basement membrane and has the function of enhancing cell adhesion and proliferation to substrates. Multiple peptide sequences have been identified as the active site of cell adhesion, one of which is Tyr-Ile-Gly-Ser-Arg (YIGSR) [17]. YIGSR adheres to various epithelial cells with laminin receptors. SF, in which YIGSR is introduced into the H chain, has been confirmed to have a higher cell adhesion activity and longer cell migration distance for vascular endothelial cells and vascular smooth muscle cells than normal-type SF. Additionally, the elongation of endothelial cells was promoted in an experiment in which a small-diameter silk artificial vascular graft made of SF containing YIGSR was implanted into the abdominal aorta of rats [18]. Due to their relatively low cost, good stability, and ease of synthesis, these peptides have been used and many studied as an effective strategy for functionalizing graft materials [19].

Transgenic SF (TGSF), into which the three types of peptide sequences described above are introduced, is expected to have desirable properties for small-diameter artificial vascular grafts. This study, as an effort toward clinical application, evaluated the *in vivo* reaction early after implantation when using genetically modified SF introduced with three types of peptide sequences as a coating and examined its effectiveness.

2. Materials and Methods

2.1. Preparation of Small-Diameter Artificial Vascular Graft Made of Three Types of TGSF Graft

The TGSF graft was prepared using the same method as Saotome et al. [20]. TGSF was obtained from silkworms injected with vectors containing VEGF, REDV, and YIGSR sequences [21]. A small-diameter artificial vascular graft with a diameter of 1.5 mm and a length of 30 mm was fabricated using normal-type SF by double-raschel knitting using a machine (HDR16-EL) manufactured by Fukui Warp Knitting Co., Ltd. (Fukui, Japan). Then,

a 2.5% (*w/v*) solution of each of VEGF-, REDV-, and YIGSR-introduced TGSF was mixed with an equal weight of glycerin to prepare a solution. The vascular graft base prepared by the double-raschel knitting described above was immersed in the solution for 30 min to allow it to permeate the entire surface. This base was passed through a vinyl chloride rod (1.5 mm), placed under reduced pressure (0.005 MPa) to prevent air from entering the base, and frozen overnight at $-20\text{ }^{\circ}\text{C}$. Afterward, it was thawed in water for 3 days, glycerin was removed, and autoclave sterilization ($120\text{ }^{\circ}\text{C}$, 20 min) was performed. Glycerin removal was confirmed using ATR-FTIR (FT/IR-4100, JASCO, Tokyo, Japan) after drying the artificial vascular graft.

2.2. Animals

This *in vivo* study used 36 Sprague-Dawley rats (Charles Laboratories, Yokohama, Japan). All experimental procedures and protocols were approved by the Tokyo University of Agriculture and Technology (TUAT; approval No. 30–94). The rats were managed and cared for following the standards established by the TUAT and described in its “Guide for the Care and Use of Laboratory Animals”.

2.3. TGSF Implantation in Rats

Three types of TGSF grafts (length: 30 mm, inner diameter: 1.5 mm) were implanted into the abdominal aorta of 36 rats under a stereoscopic microscope (LEICA M60; Leica Microsystems, Tokyo, Japan) [22]. Each TGSF was implanted in 12 rats and was removed from 6 rats 2 weeks after implantation and from the remaining 6 rats 4 weeks after implantation. The rats were anesthetized with intraperitoneal pentobarbital (50 mg/kg of body weight). The abdominal aorta was carefully exposed, and the aortic branches in this segment were ligated. The aorta was removed and replaced with grafts with an end-to-end anastomosis using 9–0 monofilament nylon sutures (Bear Medic Corporation, Tokyo, Japan). The distal and, subsequently, the proximal vascular clamps were slowly removed, and flow was restored through the grafts.

2.4. Histopathological Examination

The rats were anesthetized, and the diaphragm was cut open to secure the visual field after the implantation period had elapsed. After cutting the posterior vena cava, 0.9% saline solution was immediately injected from the left ventricle for perfusion. The grafts were carefully removed together with the surrounding tissue. The central part of the graft was cut longitudinally (approximately 10 mm) and cut 4 mm transversely toward the cranial and caudal side from the central part. The sutured parts of the remaining native blood vessel and artificial vascular graft were cut transversely (6 mm each). Ethanol was used to fix these samples for histological examination. Fixed samples were embedded in paraffin and stained with hematoxylin and eosin (HE) and Sirius red. Sections for immunohistochemical staining were incubated with primary antibodies, including α -smooth muscle actin (α -SMA: clone1A4; Sigma-Aldrich Inc., St. Louis, MO, USA) and CD31 anti-rat antibody (BD Biosciences Inc., San Jose, CA, USA). N-Histofine Simple Stain Rat MAX-PO (Nichirei Biosciences Inc., Tokyo, Japan) was used to incubate these samples. Subsequently, the ImmPACT DAB Peroxidase Substrate Kit (Vector Laboratories Inc., Newark, CA, USA) was used for color development.

2.5. Imaging and Statistical Analysis

The All-in-One fluorescence microscope (Keyence BZ-9000, Keyence, Osaka, Japan) was used to visualize the biological reactions in the stained specimens. The collagen fiber area in the graft stained with Sirius red staining was measured, and the tissue infiltration rate was calculated from the ratio to the area of the TGSF graft. The graft area was measured by combining the graft layer and the intima layer. The collagen fiber area was defined as the collagen fiber area observed within the TGSF graft area. The TGSF graft diameter was calculated by dividing the graft lumen circumference by the circumference

ratio. The lumen circumference was measured by tracking the lumen surface freehand. The endothelialization rate was calculated by measuring the distance of the vascular endothelium stained by CD31 immunostaining and calculating the endothelialization rate from the ratio to the graft's long axis length. Data are presented as mean standard error. One-way analysis of variance was used to compare the means, followed by the Bonferroni post-hoc test. The commercial statistics software package GraphPad Prism (Version 5.0a, San Diego, CA, USA) was used for data analysis. Statistical significance was defined as a p -value of <0.05 .

3. Results

3.1. In Vivo Experiment

No fraying was observed at the sutured site during the graft implantation. Additionally, complications, such as uncontrollable bleeding from grafts, were not observed in any coating. The blood flow blockage time was approximately 30–45 min, and the implantation time was approximately 45–60 min. Additionally, the rats survived until the scheduled removal date. Abnormalities, such as aneurysm or graft rupture at the anastomotic site, were observed as a macroscopic graft observation upon removal. All grafts were covered with a layer of adipose and connective tissues 2 weeks after implantation. Additionally, graft release from the surrounding tissue was easy (Figure 1). All cases demonstrated that no occlusion occurred, and thrombus adhesion was not observed on the luminal graft surface.

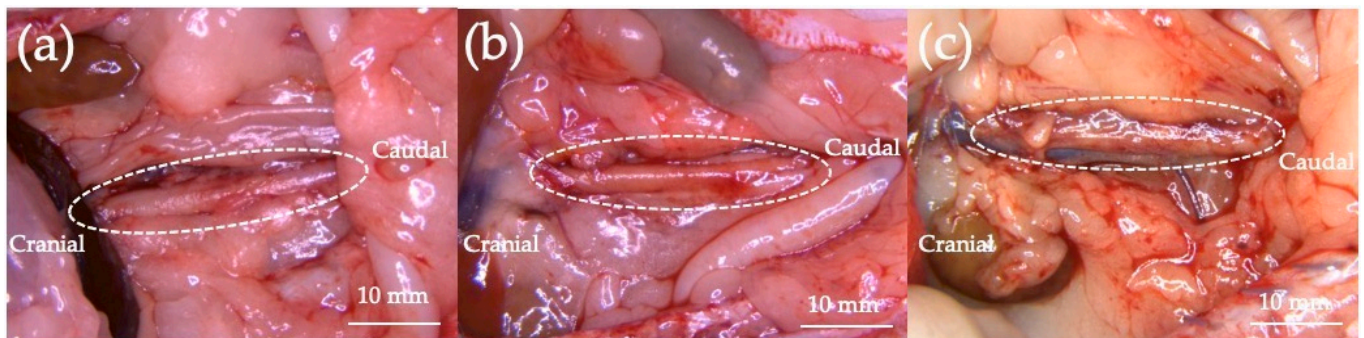


Figure 1. Photograph of the VEGF (a), REDV (b), and YIGSR graft (c) 4 weeks after implantation. Kinks or aneurysms were not observed in any grafts. The scale bar represents 10 mm.

3.2. Histopathologic Examination

HE images revealed inflammatory cells, including neutrophils, lymphocytes, macrophages, and fibroblasts, around and inside the three types of TGSF grafts in the samples obtained at 2 weeks after implantation. Inflammatory cells were observed to fill between the fibers of the graft base 4 weeks after implantation. The lumen of these grafts was slightly narrowed but not occluded. HE-stained images revealed the presence of a thick layer along the luminal surface of the grafts for all TGSF grafts. These structures consisted of smooth muscle cells, elastic fibers, and endothelial cells. Differences in the thickness of these layers were not observed among the three types of TGSF grafts (Figure 2). Additionally, no significant difference was found in lumen diameter in the three types of TGSF graft group at 2 and 4 weeks after implantation (Figure 2p).

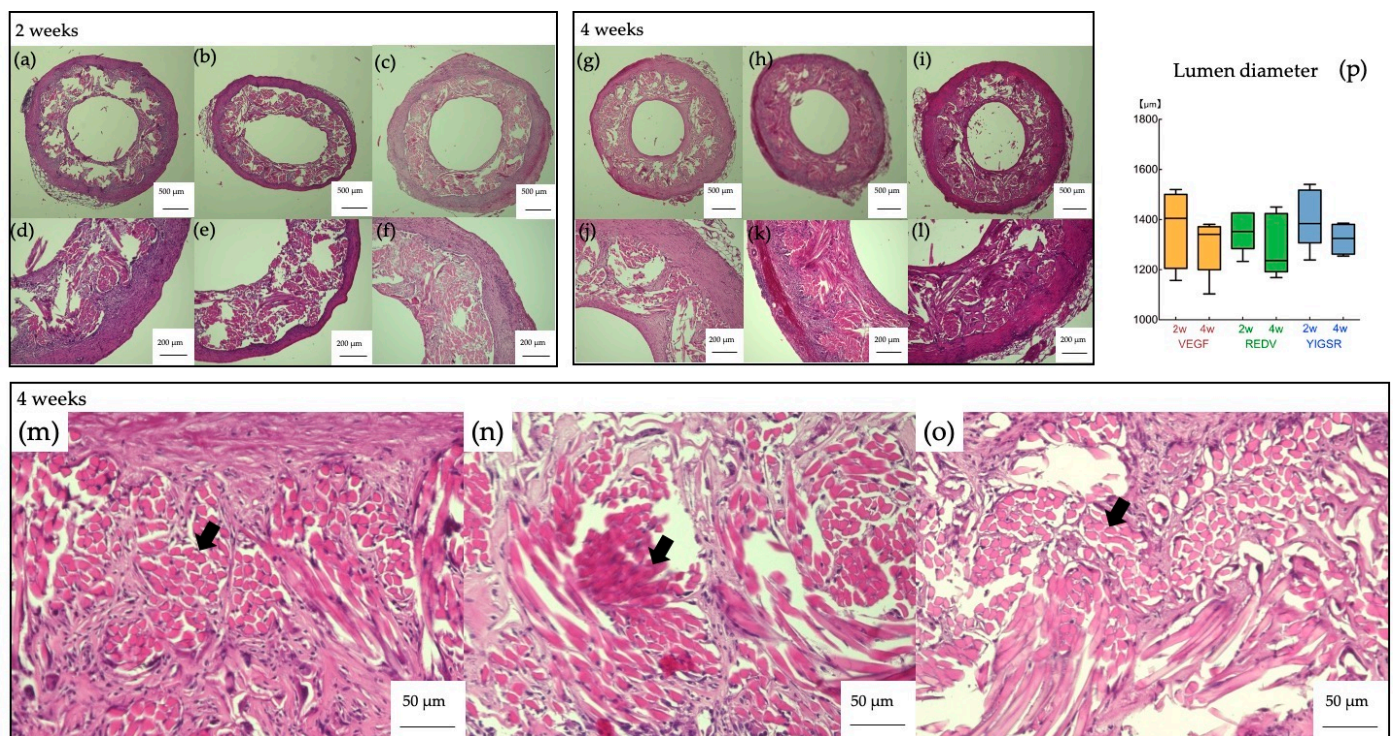


Figure 2. Histological cross-section images of HE staining 2 weeks after implantation in (a) VEGF, (b) REDV, and (c) YIGSR grafts and higher magnification in (d) VEGF, (e) REDV, and (f) YIGSR grafts. Histological cross-section images of HE staining 4 weeks after implantation in (g) VEGF, (h) REDV, and (i) YIGSR grafts and higher magnification in (j) VEGF, (k) REDV, and (l) YIGSR grafts. Histological images of HE staining 4 weeks after implantation and higher magnification in (m) VEGF, (n) REDV, and (o) YIGSR grafts. Inflammatory cells were observed to fill between the fibers of the graft base 4 weeks after implantation. The black arrows indicate silk fibers. The scale bar represents 500 μm in (a–c,g–i), 200 μm in (d–f,j–l), and 50 μm in (m–o). (p) Lumen diameter was calculated from the HE staining results. No significant difference was observed in any transgenic silk fibroin grafts at any period.

Sirius-red-stained images revealed that collagenous fibers were gathered around the graft. The collagen fibers were confirmed to mainly gather on the outside of the graft 2 weeks after implantation and partly infiltrated into the inside of the graft. The amount of collagen fiber inside the graft increased and was confirmed as a layer on the innermost side of the graft 4 weeks after implantation. These results revealed similar trends for the three types of TGSF grafts (Figure 3).

The comparison of the tissue infiltration rate revealed no significant difference in the tissue infiltration rate between any groups 2 weeks after implantation. The tissue infiltration rates of VEGF and REDV were $31.4\% \pm 9.0\%$ and $34.5\% \pm 6.6\%$ at 4 weeks after implantation, respectively, and more collagen fibers were confirmed to be infiltrated compared to $21.09\% \pm 2.17\%$ of YIGSR. Additionally, a significant increase in the tissue infiltration rate was observed in REDV 2 weeks and 4 weeks after implantation (Figure 3g).

α -SMA stained images revealed that smooth muscle cells were gathered outside the three types of TGSF grafts. A thin smooth muscle cell layer was observed in the lumen of VEGF and REDV 2 weeks after implantation, but only a partial smooth muscle cell layer was observed on the luminal surface of YIGSR. A thick layer of smooth muscle cells was observed in the innermost lumen of all TGSF grafts 4 weeks after implantation (Figure 4).

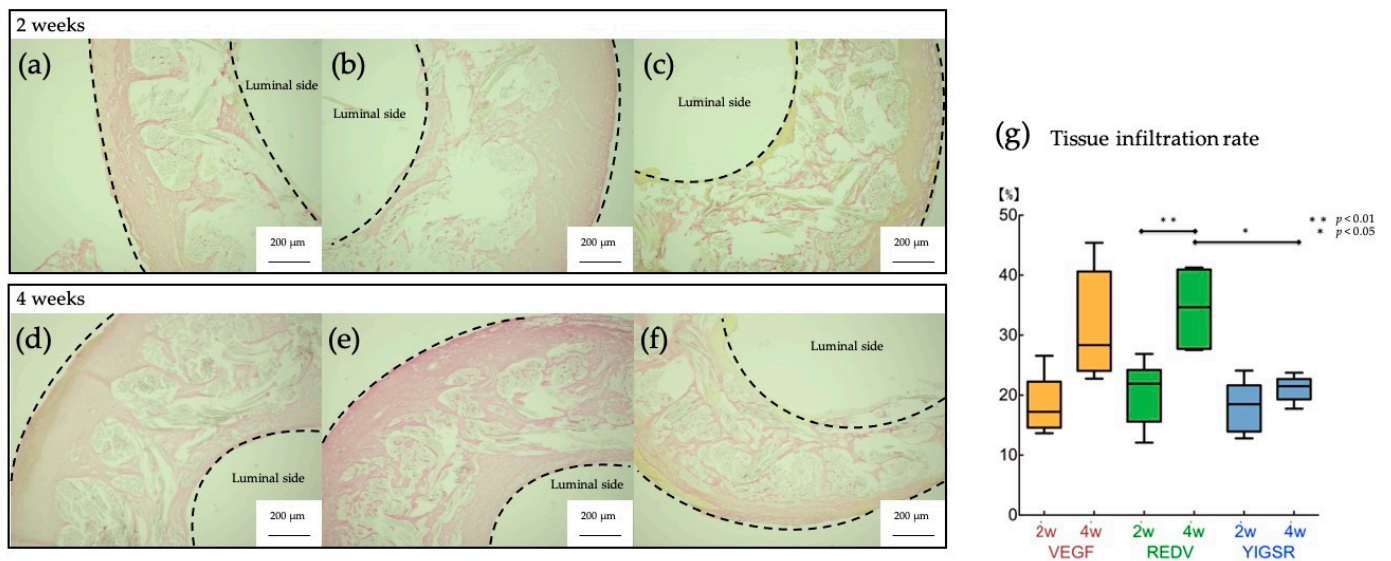


Figure 3. Histological cross-section images of Sirius red staining 2 weeks after implantation in (a) VEGF, (b) REDV, and (c) YIGSR grafts and 4 weeks after implantation in (d) VEGF, (e) REDV, and (f) YIGSR grafts. Collagen fibers (pink color) were mainly gathered on the outer circumference and inside the graft 2 weeks after implantation, and they could also be confirmed on the inner circumference of the graft 4 weeks after implantation. The black dotted lines indicate the grafts. The scale bar represents 200 μ m (a–f). (g) Tissue infiltration rate calculated from Sirius red staining results. No difference was observed among the three types of transgenic grafts 2 weeks after implantation, but VEGF and REDV grafts demonstrated increased tissue infiltration rates 4 weeks after implantation.

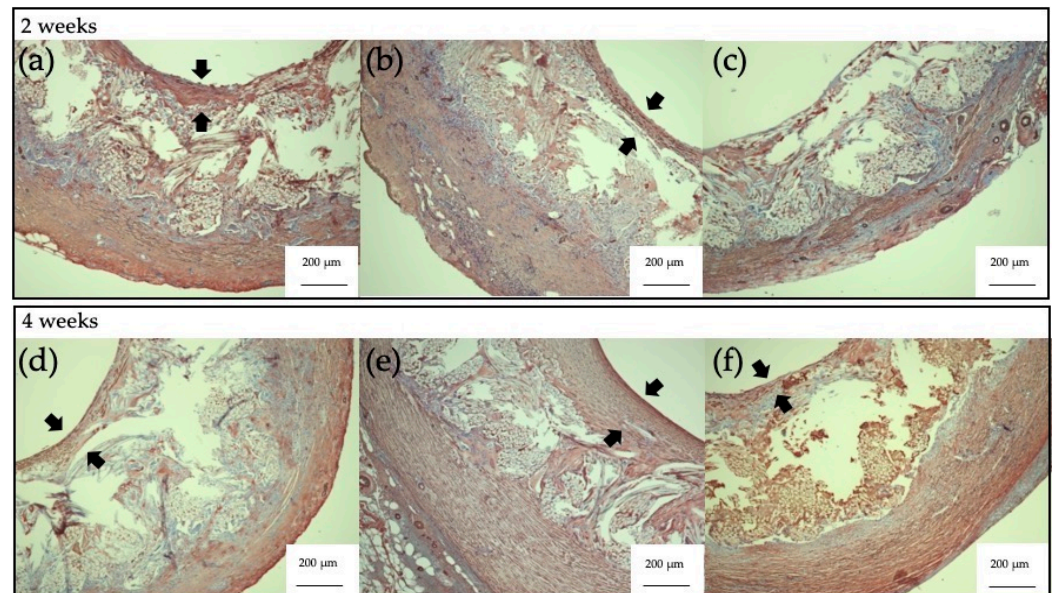


Figure 4. Histological cross-section images of α -SMA staining 2 weeks after implantation in (a) VEGF, (b) REDV, and (c) YIGSR grafts and 4 weeks after implantation in (d) VEGF, (e) REDV, and (f) YIGSR grafts. VEGF and REDV grafts demonstrated a thin smooth muscle cell layer (arrow) on the luminal surface 2 weeks after implantation, while the YIGSR graft demonstrated an intima but only a few smooth muscle cells. VEGF and REDV grafts demonstrated the formation of a thick intima mainly composed of smooth muscle cells 4 weeks after implantation, whereas YIGSR grafts formed a partial or thin smooth muscle cell layer. The scale bar represents 200 μ m (a–f).

CD31-stained images confirmed whether vascular endothelial cells covered the luminal surface of the graft. No vascular endothelial cells could be confirmed in the central part of the graft 2 weeks after implantation, but they could be confirmed in the craniocaudal region from the position. VEGF and REDV demonstrated continuous endothelialization in the center of the graft 4 weeks after implantation. Endothelialization of the central part of the graft was hardly observed in YIGSR (Figure 5). The endothelialization rate was compared between the three types of TGSF graft groups but revealed no significant difference. REDV had the highest endothelialization rate, followed by VEGF and then YIGSR (Figure 5d).

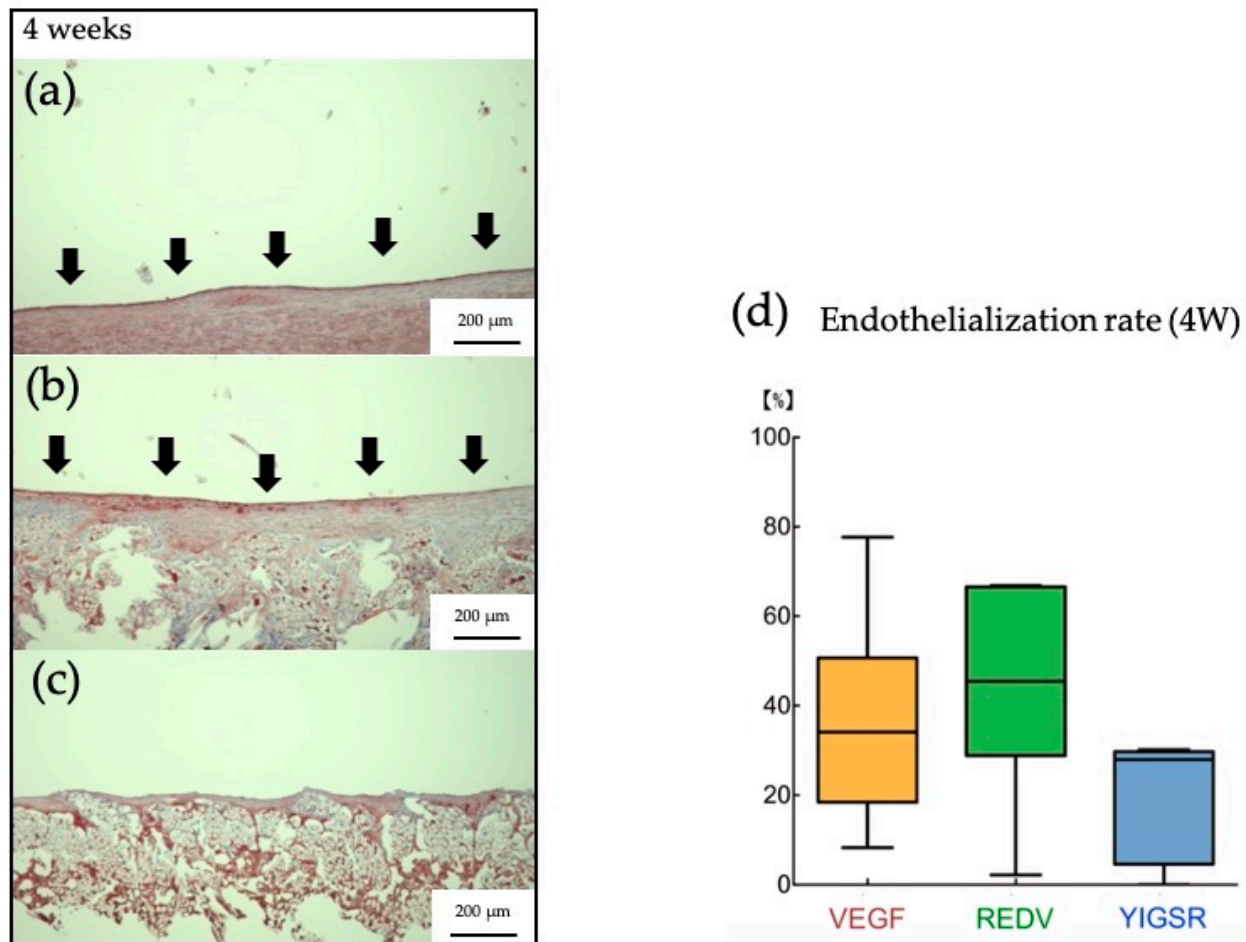


Figure 5. Histological longitudinal images of CD31 staining of the central part of the graft 4 weeks after implantation in (a) VEGF, (b) REDV, and (c) YIGSR grafts. VEGF and REDV demonstrated the appearance of continuous vascular endothelial cells (arrows) in the center of the graft, but YIGSR demonstrated no or only partial appearance. The scale bar represents 200 μm (a–c). (d) Endothelialization rate calculated from the CD31 immunostaining results 4 weeks after implantation. REDV graft tended to have the highest endothelialization rate but with no significant difference among the three types of transgenic silk fibroin grafts.

4. Discussion

SF has a long history of biocompatibility, having been used as a surgical suture for many years [23–26]. SF is known to be biodegradable in vivo, and its shape and properties can be controlled by various processing methods [27–29]. Additionally, one of the characteristics of SF is its genetic modifiability, and new functions can be acquired by introducing genes into silkworms [30–32]. This technique allows the incorporation of VEGF into the SF of bases of the artificial vascular graft and hastening endothelialization

after implantation [20,33]. Here, we examined the possibility of early endothelialization by incorporating VEGF, REDV, and YIGSR factors into the SF of the coating part.

Endothelialization was observed in VEGF and REDV, which have properties that act specifically on vascular endothelial cells and progenitor cells, but endothelialization was hardly confirmed in YIGSR, which is non-specific, even 4 weeks after implantation. Artificial vascular graft endothelialization requires the infiltration of microvessels accompanying tissue invasion [34]. Therefore, endothelialization was not confirmed in YIGSR, where the tissue infiltration rate of collagen fibers was low. In vitro experiments in which YIGSR was immobilized on glass revealed its adhesiveness to fibroblasts [35], but microvascularization that allows fibroblasts to engraft may not have occurred sufficiently in this study. REDV and VEGF tended to undergo more endothelialization than YIGSR, although no statistically significant difference was observed in the endothelialization rate. REDV and VEGF are sequences specific to vascular endothelial cells or vascular endothelial cell progenitor cells, and the difference in smooth muscle cell aggregation is thought to be one of the reasons for this difference. α -SMA staining revealed that REDV and VEGF formed a thicker smooth muscle cell layer than YIGSR. The formation of an intima by vascular smooth muscle cells is necessary for artificial vascular graft endothelialization because endothelialization of blood vessels requires support by vascular smooth muscle cells [36,37]. REDV captures vascular endothelial progenitor cells in the early post-transplantation period, and VEGF promotes vascular endothelial cell proliferation and induces angiogenesis. These grafts may have secreted PDGF from vascular endothelial cells early after implantation. PDGF is secreted from vascular endothelial cells, and it promoted mesenchymal cell proliferation and migration, including smooth muscle cells [38,39]. Additionally, the insufficient formation of the smooth muscle layer, which is the foundation of endothelialization, was considered the reason why continuous endothelialization could not be confirmed in YIGSR, which has the least smooth muscle cell aggregation. A previous study has reported that modification of YIGSR enhanced smooth muscle cell migration activity [18]. However, remodeling to autologous tissue could not be confirmed in YIGSR 4 weeks after implantation in this study. It was considered the reason that the original function of YIGSR changed after introducing YIGSR into the SF of the coating or that a sufficient amount of YIGSR was not expressed.

Endothelialization is possible even in a 3 cm graft 4 weeks after implantation. In the past, our group has confirmed normal-type silk fibroin as a coating and implanted it into the abdominal aorta of rats; the central part of the artificial vascular graft was covered with vascular endothelial cells at 3 months after implantation [22]. These results suggest that the coating using TG SF used in this experiment can contribute to remodeling to autologous tissue earlier after implantation than the coating using normal-type SF. Endothelialization due to vascular endothelial cell migration from the graft anastomosis is approximately 1 cm [33,40]. Therefore, the endothelialization of the central part of the graft with a length of ≥ 2 cm is attributed to the proliferation of captured vascular endothelial cells and vascular endothelial cell progenitor cells in the blood [41]. Endothelialization was confirmed at the center of the 3 cm long graft, indicating that the cell-adhesive peptide sequence introduced in this study captured these cells and promoted proliferation.

The physical properties of the TG SF grafts fabricated in this study were not tested. The same degree of physical properties was thought to be maintained because the same manufacturing method was used as the substrate used in the previous research [22]. No uncontrolled bleeding or suture dehiscence was observed in any of the implanted cases, and no aneurysm formation was confirmed upon extraction, indicating that sufficient strength was maintained. We have created small-diameter artificial vascular grafts with a double-raschel knitted base coated with an aqueous SF solution [42]. The base of the artificial vascular grafts alone cannot be used because a large amount of blood has leaked from the gaps in the base mesh. However, cell adhesion and infiltration will not occur after transplantation if the interstices of the artificial vascular grafts are completely embedded, resulting in insufficient remodeling [43]. Therefore, the coating material must be eluted at an appropriate time after implantation.

This study confirmed endothelialization 4 weeks after implantation by TGSF coating with VEGF and REDV introduced into the H chain. A previous study revealed no endothelialization in normal-type SF-coated vascular grafts 4 weeks after implantation [20]. The usefulness of TGSF coating for clinical application has been clarified because small-diameter artificial vascular grafts require endothelialization at an early stage after implantation. However, to what extent VEGF, REDV, and YIGSR factors are present in the SF of the coating part has not been demonstrated in this study. In the future, it is necessary to validate whether the presence of the VEGF, REDV, and YIGSR are contained in the SF of the coating part. In addition, investigating physical properties and the optimal coating concentration for practical application is necessary.

5. Conclusions

This study revealed that early endothelialization can be realized using TGSF for coating. Additionally, the degree of endothelialization and tissue infiltration indicate that VEGF and REDV were the sequences that showed the most effect on SF small-diameter artificial vascular grafts among the three peptide sequences used this time.

Author Contributions: Conceptualization, T.T. and T.A.; methodology, T.T. and S.H.; software, R.T.; validation, H.H.; formal analysis, H.M.E.-H.; investigation, S.H.; writing—original draft preparation, T.T., S.H. and R.T.; writing—review and editing, T.T. and T.A. All authors have read and agreed to the published version of the manuscript.

Funding: This research was funded by Japan Society for the Promotion of Science (JSPS) KAKENHI, Grant-in-Aid for Scientific Research (C), grant number JP20K12643.

Institutional Review Board Statement: The study was conducted according to the guidelines of the Declaration of Helsinki and approved by the Institutional Review Board (or Ethics Committee) of Tokyo University of Agriculture and Technology (approval No. R30–94).

Informed Consent Statement: Not applicable.

Data Availability Statement: Data is contained within the article.

Conflicts of Interest: The authors declare no conflict of interest.

References

1. Pashneh-Tala, S.; MacNeil, S.; Claeysens, F. The Tissue-Engineered Vascular Graft—Past, Present, and Future. *Tissue Eng. Part B Rev.* **2016**, *22*, 68–100. [[CrossRef](#)] [[PubMed](#)]
2. Liu, S.S.; Dong, C.F.; Lu, G.Z.; Lu, Q.; Li, Z.X.; Kaplan, D.L.; Zhu, H.S. Bilayered vascular grafts based on silk proteins. *Acta Biomater.* **2013**, *9*, 8991–9003. [[CrossRef](#)] [[PubMed](#)]
3. Seib, F.P.; Herklotz, M.; Burke, K.A.; Maitz, M.F.; Werner, C.; Kaplan, D.L. Multifunctional silk-heparin biomaterials for vascular tissue engineering applications. *Biomaterials* **2014**, *35*, 83–91. [[CrossRef](#)] [[PubMed](#)]
4. Baguneid, M.S.; Seifalian, A.M.; Salacinski, H.J.; Murray, D.; Hamilton, G.; Walker, M.G. Tissue engineering of blood vessels. *Brit. J. Surg.* **2006**, *93*, 282–290. [[CrossRef](#)] [[PubMed](#)]
5. Liu, H.F.; Ding, X.L.; Bi, Y.X.; Gong, X.H.; Li, X.M.; Zhou, G.; Fan, Y.B. In Vitro Evaluation of Combined Sulfated Silk Fibroin Scaffolds for Vascular Cell Growth. *Macromol. Biosci.* **2013**, *13*, 755–766. [[CrossRef](#)]
6. Motlagh, D.; Allen, J.; Hoshi, R.; Yang, J.; Lui, K.; Ameer, G. Hemocompatibility evaluation of poly(diols citrate) in vitro for vascular tissue engineering. *J. Biomed. Mater. Res. A* **2007**, *82a*, 907–916. [[CrossRef](#)]
7. Nomi, M.; Atala, A.; De Coppi, P.; Soker, S. Principles of neovascularization for tissue engineering. *Mol. Aspects Med.* **2002**, *23*, 463–483. [[CrossRef](#)]
8. Enomoto, S.; Sumi, M.; Kajimoto, K.; Nakazawa, Y.; Takahashi, R.; Takabayashi, C.; Asakura, T.; Sata, M. Long-term patency of small-diameter vascular graft made from fibroin, a silk-based biodegradable material. *J. Vasc. Surg.* **2010**, *51*, 155–164. [[CrossRef](#)]
9. Fukayama, T.; Takagi, K.; Tanaka, R.; Hatakeyama, Y.; Aytemiz, D.; Suzuki, Y.; Asakura, T. Biological Reaction to Small-Diameter Vascular Grafts Made of Silk Fibroin Implanted in the Abdominal Aortae of Rats. *Ann. Vasc. Surg.* **2015**, *29*, 341–352. [[CrossRef](#)]
10. Losi, P.; Lombardi, S.; Briganti, E.; Soldani, G. Luminal surface microgeometry affects platelet adhesion in small-diameter synthetic grafts. *Biomaterials* **2004**, *25*, 4447–4455. [[CrossRef](#)]
11. Knetsch, M.L.W.; Koole, L.H. VEGF-E enhances endothelialization and inhibits thrombus formation on polymeric surfaces. *J. Biomed. Mater. Res. A* **2010**, *93a*, 77–85. [[CrossRef](#)]

12. Dorafshar, A.H.; Angle, N.; Bryer-Ash, M.; Huang, D.S.; Farooq, M.M.; Gelabert, H.A.; Freischlag, J.A. Vascular endothelial growth factor inhibits mitogen-induced vascular smooth muscle cell proliferation. *J. Surg. Res.* **2003**, *114*, 179–186. [[CrossRef](#)] [[PubMed](#)]
13. Swanson, N.; Hogrefe, K.; Javed, Q.; Gershlick, A.H. In vitro evaluation of vascular endothelial growth factor (VEGF)-eluting stents. *Int. J. Cardiol.* **2003**, *92*, 247–251. [[CrossRef](#)] [[PubMed](#)]
14. Randone, B.; Cavallaro, G.; Polistena, A.; Cucina, A.; Coluccia, P.; Graziano, P.; Cavallaro, A. Dual role of VEGF in pretreated experimental ePTFE arterial grafts. *J. Surg. Res.* **2005**, *127*, 70–79. [[CrossRef](#)]
15. Zhang, B.; Qin, Y.M.; Wang, Y.B. A nitric oxide-eluting and REDV peptide-conjugated coating promotes vascular healing. *Biomaterials* **2022**, *284*, 121478. [[CrossRef](#)]
16. Mahara, A.; Somekawa, S.; Kobayashi, N.; Hirano, Y.; Kimura, Y.; Fujisato, T.; Yamaoka, T. Tissue-engineered acellular small diameter long-bypass grafts with neointima-inducing activity. *Biomaterials* **2015**, *58*, 54–62. [[CrossRef](#)]
17. Wang, P.Y.; Wu, T.H.; Tsai, W.B.; Kuo, W.H.; Wang, M.J. Grooved PLGA films incorporated with RGD/YIGSR peptides for potential application on skeletal muscle tissue engineering. *Colloid Surf. B* **2013**, *110*, 88–95. [[CrossRef](#)] [[PubMed](#)]
18. Asakura, T.; Isozaki, M.; Saotome, T.; Tatematsu, K.I.; Sezutsu, H.; Kuwabara, N.; Nakazawa, Y. Recombinant silk fibroin incorporated cell-adhesive sequences produced by transgenic silkworm as a possible candidate for use in vascular graft. *J. Mater. Chem. B* **2014**, *2*, 7375–7383. [[CrossRef](#)]
19. Peng, G.; Yao, D.Y.; Niu, Y.M.; Liu, H.F.; Fan, Y.B. Surface Modification of Multiple Bioactive Peptides to Improve Endothelialization of Vascular Grafts. *Macromol. Biosci.* **2019**, *19*, 1800368. [[CrossRef](#)] [[PubMed](#)]
20. Saotome, T.; Hayashi, H.; Tanaka, R.; Kinugasa, A.; Uesugi, S.; Tatematsu, K.; Sezutsu, H.; Kuwabara, N.; Asakura, T. Introduction of VEGF or RGD sequences improves revascularization properties of Bombyx mori silk fibroin produced by transgenic silkworm. *J. Mater. Chem. B* **2015**, *3*, 7109–7116. [[CrossRef](#)]
21. Iizuka, T.; Sezutsu, H.; Tatematsu, K.; Kobayashi, I.; Yonemura, N.; Uchino, K.; Nakajima, K.; Kojima, K.; Takabayashi, C.; Machii, H.; et al. Colored Fluorescent Silk Made by Transgenic Silkworms. *Adv. Funct. Mater.* **2013**, *23*, 5232–5239. [[CrossRef](#)]
22. Tanaka, T.; Uemura, A.; Tanaka, R.; Tasei, Y.; Asakura, T. Comparison of the knitted silk vascular grafts coated with fibroin sponges prepared using glycerin, poly(ethylene glycol diglycidyl ether) and poly(ethylene glycol) as porogens. *J. Biomater. Appl.* **2018**, *32*, 1239–1252. [[CrossRef](#)] [[PubMed](#)]
23. Altman, G.H.; Diaz, F.; Jakuba, C.; Calabro, T.; Horan, R.L.; Chen, J.S.; Lu, H.; Richmond, J.; Kaplan, D.L. Silk-based biomaterials. *Biomaterials* **2003**, *24*, 401–416. [[CrossRef](#)] [[PubMed](#)]
24. Vepari, C.; Kaplan, D.L. Silk as a biomaterial. *Prog. Polym. Sci.* **2007**, *32*, 991–1007. [[CrossRef](#)]
25. Thurber, A.E.; Omenetto, F.G.; Kaplan, D.L. In vivo bioresponses to silk proteins. *Biomaterials* **2015**, *71*, 145–157. [[CrossRef](#)] [[PubMed](#)]
26. Aigner, T.B.; DeSimone, E.; Scheibel, T. Biomedical Applications of Recombinant Silk-Based Materials. *Adv. Mater.* **2018**, *30*, 1704636. [[CrossRef](#)]
27. Horan, R.L.; Antle, K.; Collette, A.L.; Huang, Y.Z.; Huang, J.; Moreau, J.E.; Volloch, V.; Kaplan, D.L.; Altman, G.H. In vitro degradation of silk fibroin. *Biomaterials* **2005**, *26*, 3385–3393. [[CrossRef](#)]
28. Numata, K.; Cebe, P.; Kaplan, D.L. Mechanism of enzymatic degradation of beta-sheet crystals. *Biomaterials* **2010**, *31*, 2926–2933. [[CrossRef](#)] [[PubMed](#)]
29. Guo, C.C.; Li, C.M.; Kaplan, D.L. Enzymatic Degradation of Bombyx mori Silk Materials: A Review. *Biomacromolecules* **2020**, *21*, 1678–1686. [[CrossRef](#)]
30. Imamura, M.; Nakai, J.; Inoue, S.; Quan, G.X.; Kanda, T.; Tamura, T. Targeted gene expression using the GAL4/UAS system in the silkworm Bombyx mori. *Genetics* **2003**, *165*, 1329–1340. [[CrossRef](#)]
31. Inoue, S.; Kanda, T.; Imamura, M.; Quan, G.X.; Kojima, K.; Tanaka, H.; Tomita, M.; Hino, R.; Yoshizato, K.; Mizuno, S.; et al. A fibroin secretion-deficient silkworm mutants Nd-s(D), provides an efficient system for producing recombinant proteins. *Insect Biochem. Mol.* **2005**, *35*, 51–59. [[CrossRef](#)]
32. Tomita, M.; Munetsuna, H.; Sato, T.; Adachi, T.; Hino, R.; Hayashi, M.; Shimizu, K.; Nakamura, N.; Tamura, T.; Yoshizato, K. Transgenic silkworms produce recombinant human type III procollagen in cocoons. *Nat. Biotechnol.* **2003**, *21*, 52–56. [[CrossRef](#)] [[PubMed](#)]
33. Fukayama, T.; Ozai, Y.; Shimokawatoko, H.; Kimura, Y.; Aytemiz, D.; Tanaka, R.; Machida, N.; Asakura, T. Evaluation of endothelialization in the center part of graft using 3 cm vascular grafts implanted in the abdominal aortae of the rat. *J. Artif. Organs* **2017**, *20*, 221–229. [[CrossRef](#)] [[PubMed](#)]
34. Pawlowski, K.J.; Rittgers, S.E.; Schmidt, S.P.; Bowlin, G.L. Endothelial cell seeding of polymeric vascular grafts. *Front. Biosci.-Landmark* **2004**, *9*, 1412–1421. [[CrossRef](#)]
35. Massia, S.P.; Hubbell, J.A. Vascular Endothelial-Cell Adhesion and Spreading Promoted by the Peptide Redv of the Iiics Region of Plasma Fibronectin Is Mediated by Integrin Alpha-4-Beta-1. *J. Biol. Chem.* **1992**, *267*, 14019–14026. [[CrossRef](#)]
36. Richardson, T.P.; Peters, M.C.; Ennett, A.B.; Mooney, D.J. Polymeric system for dual growth factor delivery. *Nat. Biotechnol.* **2001**, *19*, 1029–1034. [[CrossRef](#)] [[PubMed](#)]
37. Yancopoulos, G.D.; Davis, S.; Gale, N.W.; Rudge, J.S.; Wiegand, S.J.; Holash, J. Vascular-specific growth factors and blood vessel formation. *Nature* **2000**, *407*, 242–248. [[CrossRef](#)]

38. Conway, E.M.; Collen, D.; Carmeliet, P. Molecular mechanisms of blood vessel growth. *Cardiovasc. Res.* **2001**, *49*, 507–521. [[CrossRef](#)]
39. Zhang, H.; Jia, X.L.; Han, F.X.; Zhao, J.; Zhao, Y.H.; Fan, Y.B.; Yuan, X.Y. Dual-delivery of VEGF and PDGF by double-layered electrospun membranes for blood vessel regeneration. *Biomaterials* **2013**, *34*, 2202–2212. [[CrossRef](#)]
40. Noishiki, Y.; Yamane, Y.; Tomizawa, Y.; Matsumoto, A. Transplantation of Autologous Tissue Fragments into an E-Ptfe Graft with Long Fibrils. *Artif. Organs* **1995**, *19*, 17–26. [[CrossRef](#)]
41. Byrom, M.J.; Bannon, P.G.; White, G.H.; Ng, M.K.C. Animal models for the assessment of novel vascular conduits. *J. Vasc. Surg.* **2010**, *52*, 176–195. [[CrossRef](#)] [[PubMed](#)]
42. Yagi, T.; Sato, M.; Nakazawa, Y.; Tanaka, K.; Sata, M.; Itoh, K.; Takagi, Y.; Asakura, T. Preparation of double-raschel knitted silk vascular grafts and evaluation of short-term function in a rat abdominal aorta. *J. Artif. Organs* **2011**, *14*, 89–99. [[CrossRef](#)] [[PubMed](#)]
43. Tanaka, T.; Tanaka, R.; Ogawa, Y.; Takagi, Y.; Asakura, T. Development of Small-diameter Polyester Vascular Grafts Coated with Silk Fibroin Sponge. *Organogenesis* **2020**, *16*, 1–13. [[CrossRef](#)] [[PubMed](#)]

Disclaimer/Publisher’s Note: The statements, opinions and data contained in all publications are solely those of the individual author(s) and contributor(s) and not of MDPI and/or the editor(s). MDPI and/or the editor(s) disclaim responsibility for any injury to people or property resulting from any ideas, methods, instructions or products referred to in the content.